

Modeling Blood Flow in a Brain Tumor Treated Concurrently with Radiotherapy and Chemotherapy

Ranadhir Roy*, Daniel N Riahi

Mathematics Department, University of Texas-Pan American, Edinburg, Texas

*Corresponding author: rroy@utpa.edu

Received July 08, 2013; Revised September 27, 2013; Accepted October 06, 2013

Abstract Blood flow through a tumor plays a critical role in tumor growth and cancer therapies. Hence, fluid dynamics is an appropriate method to study blood flow through a tumor. Drug transport in the tumor interstitial depends on convection and diffusion. To investigate characteristics of blood flow through a spherical tumor, a coupled convection-diffusion models for simulating the interactions between two anti cancer drugs has been developed in this paper. This model provides the computational transportation to evaluate systematically and quantitatively the effects of interactions on the concentration within the tumor. Mathematical expressions for the spatial variations of the interstitial velocity and interstitial pressure are developed and calculated analytically, while variations of drug concentrations within a tumor are determined numerically in this paper. We determined the way interstitial pressure and velocity vary in the radial direction, which agreed with the experiments, as well as we studied the way one drug concentration changes in the presence or absence of a second drug within the tumor. We found that the concentration of a drug in the tumor could be improved in the presence of another drug in the tumor.

Keywords: brain tumor, cancer therapy, convection and diffusion, blood flow, drug concentration, fluid dynamics

Cite This Article: Ranadhir Roy, and Daniel N Riahi, "Modeling Blood Flow in a Brain Tumor Treated Concurrently with Radiotherapy and Chemotherapy." *Applied Mathematics and Physics* 1, no. 3 (2013): 67-77. doi: 10.12691/amp-1-3-4.

1. Introduction

Cancer is the second biggest cause of death in America. The most intrusive treatment is surgical removal of the tumor; however, surgery often leaves behind residual tumor cells and re-growth of these tumor cells is very common. In order to prevent the reoccurrence of tumor cells, anticancer drugs are used. Radiotherapy is a valuable post-operative treatment. Etanidazole is given by injection before radiation therapy. Etanidazole mimics oxygen, thus increasing the damaging effects of radiotherapy. This drug also makes it harder for cancer cells to repair themselves, so they die. However, many studies have been attempted to demonstrate a better outcome with the addition of chemotherapy [1]. In chemotherapy, an anti cancer drug cisplatin solution (liquid) is injected intravenously over 6 to 8 hour period. This stops or slows the growth of cancer cells. A combined radiotherapy and chemotherapy treatment can improve the survival rates [2].

A more successful cure would be the result of an efficient distribution of anticancer drug within targeted areas after tumor removal the surgery. The most noticeable limitation for anticancer drugs is their inability to reach the targeted area because of a major barrier in the brain called the blood-brain barrier, which is an area between the blood vessels and extravascular brain tissue [3]. The two most important considerations in the

effective cancer treatment, from a mathematical point of view, are drug transport to the affected area and the reaction at the tumor site. Many drugs cannot be delivered to the targeted region because of transport limitations. More than 85% of human cancers are solid and highly heterogeneous tumors, so current radiotherapy and chemotherapy treatments depend on adequate delivery of therapeutic agents to tumor sites. In fact, drug concentration is the highest in a region near vasculature, well-perfused areas and on the peripheral walls of the tumor; however, a very small amount of the drug reaches the tumor [4]. Therefore, cancer treatment would be more successful if all areas of a tumor are exposed to radiotherapy/chemotherapy agents. Otherwise, if only the outer cells of a tumor are killed, the tumor cells within will redevelop. Some researchers have shown that heterogeneities and obstructed interstitial transport effectively contribute to the non-uniform distribution of drugs in solid tumors where the interstitial pressure is very high. This high interstitial pressure limits the transport of anticancer drugs in solid tumors. Another important process in drug delivery is inward diffusion, due to the concentration gradient of the drug. Therefore, the main focus of future drug delivery modeling would be on the transport of the drug through tissues after a drug is released using the systemic administration or implantation mechanisms. Modeling in drug delivery involves different processes such as drug diffusion, convective transport through extracellular tissue, drug extravasations from blood vessels, and tissue elimination by the lymphatic

system [5]. Computational fluid dynamics is a suitable subject for understanding the mechanisms of drug delivery from the injection site to absorption by a solid tumor. Numerical simulations can provide a detailed understanding of the mechanisms of interstitial fluid transport and will help us to understand the major barriers of drug delivery to solid tumors.

There have been a number of studies about tumors, in general, [5-10] and brain tumors, in particular [11,12,13]. Important modeling works have been performed by Baxter and Jain [1-6]. They have developed a general theoretical framework for transvascular exchange, interstitial transport of fluid and macromolecules in tumors. Arifin *et al.* [14] have looked into local intratumoral drug transport in a brain tumor by employing methods of computational fluid dynamics. Sinek *et al.* [15] have presented a 2D simulation of drug delivery involving nanoparticles and their therapeutic effects on a tumoral lesion based on the convection-diffusion model developed by Zheng *et al.* [16]. Swanson *et al.* [17] have developed a model of a brain tumor consisting of both grey and white matter and have shown that chemotherapy affected the cells within the grey matter only. Powathil *et al.* [1] have described the effect of radiotherapy and TMZ (temozolomide). Eikenberry *et al.* [18] have developed a model to analyze drug delivery and a tumor's response using idealized tumor cord geometry. Their model provides detailed descriptions of blood-flow and cellular mechanics.

Even though many experimental and computational investigations on tumors have been carried out in the past, including those referenced here and many others [see references within [1-6], there is very little information available about the mechanisms of drug interactions when more than one drug is present in a patient's body. Furthermore, the presence of drugs in a patient's brain can lead to harmful side effects and interactions between drugs may damage the efficiency of drug delivery and its usefulness. In addition, anticancer drugs can also affect the normal tissues in the brain. Consequently, it is very crucial to study and understand the effects of a drug's concentration in a brain tumor in the presence of another anticancer drug; how the interaction of the two drugs can affect the overall usefulness of each drug and the harmful effects that anticancer drugs can have on the normal tissues.

Our major objective in this paper is to understand the physiology of blood flow in a solid tumor and also to investigate the effect of an anti-cancer drug on a solid tumor in the presence of another drug. There is a need to develop a mathematical model of interstitial fluid flow based on the application of the governing equations for fluid flow, i.e., the conservation laws for mass and momentum. Numerical techniques are used to solve the governing equations using appropriate boundary conditions and defined tumor geometry. First interstitial fluid pressure and velocity are calculated. We then examined the distribution of an anticancer drug within the solid tumor. Simulations of interstitial fluid transport in a homogeneous solid tumor with no necrotic core region are investigated. The resulting mathematical model should be accurate enough to include the spatial dependency of physiological parameters, such as the hydraulic conductivity and diffusion; that is, it must be able to clearly represent all the physical variations in a tumor.

Because the time scale of transport phenomena is much less than that of tumor growth, the physiological parameters can be considered time independent. For the sake of simplicity, here solid tumors are considered to be spherical.

In the present study, we developed a coupled convection-diffusion equations for unsteady and steady blood flow within the unsteady solid spherical homogeneous tumor. We developed models for both unsteady and steady systems separately. Such steady state features of the flow quantities, which can be considered as time averages of flow quantities, are reasonable under the assumption that the rate of the growth of the tumor is sufficiently small. We determined important quantities such as interstitial velocity and pressure as functions of distance from the center of the tumor, and, in addition, we determined the radial and time variations of a drug concentration in the presence or absence of another drug within such systems. To our knowledge, this is the first time a theoretical investigation has been carried out to obtain information about the mechanism of the drug interactions. Furthermore, our present investigation can help improve the understanding of transport mechanisms in tumors, which can consequently, help improve drug delivery schemes. This paper is the continuation of our previous paper [19] that investigates only steady state features of a brain tumor.

In this study, we specifically attempt to describe a brain tumor's response to a combination of both radiotherapy and chemotherapy. We found some exciting results. We detected some inter relations between radiotherapy, chemotherapy, and the physical systems as well as some mechanical causes for the decrease or increase of the drug effectiveness within the patient's brain. These can be useful as additional guiding tools for specialists and doctors to improve the chances for a patient's recovery.

2. Mathematical Model

It is well established that a solid tumor is spatially heterogeneous with large differences between different regions. A tumor contains a necrotic core at the center, and the outer region of the tumor has rapidly dividing cells with a blood supply and a large quantity of exchange vessels [20]. Drug transport in the tumor interstitium depends on convection and diffusion. The interstitial fluid pressure (IFP) is very high in solid tumors due to leaky blood vessels and lack of a lymphatic drainage. This weakens the role of convection in transcapillary and interstitial transport, thus creating a barrier for efficient drug delivery [21]. Diffusion of a drug through tumor tissues depends on the physicochemical properties of the drug and the concentration gradient. A coupled convection-diffusion model for simulating interactions between two anti cancer drugs has been developed. The basic assumptions in the mathematical model are: (i) the tumor is spherical and homogeneous, (ii) the physiological parameters are independent of time and space, (iii) the time scale for transport is small compared to the time constant for tumor growth, and (iv) the tumor is surrounded by normal tissue

In this study, we used the Darcy model to represent the flow through the porous medium and the Starling law to

describe the vascular fluid exchange and the leakiness from the vessel [10,12,22]. The Darcy model is the earliest flow transport model in porous media and there is a linear proportionality between the flow velocity and the applied pressure gradient. The fluid transport in the tumor interstitial can be described by Darcy's law through a porous medium.

$$-\nabla P + \frac{\mu}{\kappa} \mathbf{u} = 0, \quad (1a)$$

where κ is the permeability of the porous medium, P is the interstitial (tissue) fluid pressure, μ is dynamic viscosity, \mathbf{u} is interstitial fluid velocity (the average of the fluid velocity over the cross section). The mass balance equation for an incompressible fluid is that the divergence of the interstitial fluid velocity vector is zero ($\nabla \cdot \mathbf{u} = 0$). This porous media contains a tissue and vascular component. The vascular component provides a source, or sink, for both plasma fluid and tissue volume. Hence, in biological tissue, source and sinks are present; therefore, the steady state incompressible form of the continuity equation must be modified. The source and sink is based on Starling's law and the fluid production by cells due to metabolism [10]. Starling's equation refers to fluid movement across the capillary membrane that occurs as a result of filtration and is described as

$$\frac{J_V S}{V} = \frac{K_V S}{V} [P_V - P_i - \sigma_s (\pi_B - \pi_i)], \quad (1b)$$

where J_V/V is the volumetric flow rate out of the vasculature unit volume of tissue, K_V is the hydraulic conductivity of the microvascular wall, S/V is the surface area per unit volume for transport in the tumor, P_V is vascular pressure, P_i is the interstitial pressure, σ_s is the average osmotic reflection coefficient for plasma proteins, π_B is the osmotic pressure of the plasma and π_i is the osmotic pressure of the interstitial fluid.

Due to symmetry, there is no flux boundary condition at the center of the tumor [12], so that

$$\nabla \cdot \mathbf{u} = a_1 - a_2 P, \quad \frac{\partial P}{\partial r} = 0 \quad \text{at } r = 0 \quad (1c)$$

a_1 and a_2 are constants whose expressions are given in [12]

$$a_1 = \phi_B(r) = \frac{J_V S}{V} = \frac{K_V S}{V} (P_V - P_i - \sigma_s (\pi_B - \pi_i))$$

with a_1 is based on hydraulic conductivity of the macrovascular wall, vascular pressure, osmotic reflection coefficient for the plasma protein, osmotic pressures of the plasma and interstitial pressures and exchange area S/V of the blood vessels per unit volume of tissues, $a_2 = K_V S/V$.

The anticancer drug conservation equation is coupled together with the flow equation to arrive at the governing equation for the concentration field. That is, the transport of interstitial anti cancer drugs is solved using the convection and diffusion equation for porous media.

$$\frac{\partial C_1}{\partial t} + \mathbf{u} \cdot \nabla C_1 = D_1 \nabla^2 C_1 - a_3 C_1 - a_4 C_2 \quad (2a)$$

$$\frac{\partial C_2}{\partial t} + \mathbf{u} \cdot \nabla C_2 = D_2 \nabla^2 C_2 - a_5 C_1 - a_6 C_2 \quad (2b)$$

$$P = P_B \quad \text{at } r = R(t) \quad (2c)$$

$$C_i = C_{Bi} \quad \frac{\partial C_i}{\partial r} = T_i \quad \text{at } r = R(t), \quad (i=1,2) \quad (2d)$$

In equations (2a-b), the second term on the left describes the convective flux and the first term on the right describes the diffusive flux. The expression for the time-dependent radius is considered to be in the form of $R(t)$ as radius of the tumor, α as positive and small.

$$R(t) = R_0 \exp\{\varepsilon [1 - \exp(-\alpha t)]\}, \quad (3)$$

where ε is a non-dimensional small parameter ($\varepsilon \leq 1$) representing the order of magnitude of the relative growth rate of the tumor, R_0 is the constant radius of tumor in the absence of its growth and α is a constant of order of one quantity of the tumor. So α and ε represent the inverse of a time scale and provide the relative rate of growth of the tumor, initially ($t = 0$). We have assumed that the tumor growth is very slow over time. We consider, C_1 (etanidazole, a kind of radiotherapy) and C_2 (cisplatin, a kind of chemotherapy) are concentration of anticancer drugs with diffusion coefficients D_1 and D_2 , respectively. P is the interstitial pressure, k is the permeability, \mathbf{u} is the interstitial fluid velocity, and P_B is a nonzero constant. The expressions are given in Tan *et al.* [12] a_3, a_4, a_5 and a_6 are constant coefficients of source and sink terms in the concentration equation, which can be due to the presence of either one or two drugs. Source and sink terms can be due to the chemical elimination by the drug degradation in the cavity, metabolic reactions in the tumor and the normal tissue, as well as the drug gain from the blood capillaries in the tumor and tissue [19]. C_{Bi} and T_i are constants on the boundary. It should be noted that these values are obtained from references [12].

We considered the one-dimensional case of the flow system where the spatial variation is only along the radial direction and the velocity vector only has a non-zero component along the radial direction. In spherical coordinates, we have

$$\nabla^2 = \frac{1}{r^2} \frac{\partial}{\partial r} \left(r^2 \frac{\partial}{\partial r} \right), \quad \nabla = \left(\frac{\partial}{\partial r}, 0, 0 \right), \quad \mathbf{u} = (u, 0, 0) \quad (3a)$$

Using (2) in (1a-1c), we obtain

$$-\frac{\partial P}{\partial r} + \frac{\mu}{k} u = 0 \quad (3b)$$

$$\frac{\partial u}{\partial r} = a_1 - a_2 P \quad (3c)$$

$$\frac{\partial C_1}{\partial t} + u \frac{\partial C_1}{\partial r} = D_1 \left[\frac{1}{r^2} \frac{\partial}{\partial r} \left(r^2 \frac{\partial}{\partial r} \right) \right] C_1 - a_3 C_1 - a_4 C_2 \quad (3d)$$

$$\frac{\partial C_2}{\partial t} + u \frac{\partial C_2}{\partial r} = D_2 \left[\frac{1}{r^2} \frac{\partial}{\partial r} \left(r^2 \frac{\partial}{\partial r} \right) \right] C_2 - a_5 C_1 - a_6 C_2 \quad (3e)$$

$$P = P_B \text{ at } r = R(t), \quad \frac{\partial P}{\partial r} = 0 \text{ at } r = 0 \quad (3f)$$

We then apply a perturbation expansion in powers of small ε by assuming that the growth rate of increase of the tumor with respect to time is sufficiently small ($\varepsilon \ll 1$). Thus, we consider (3) to the lowest order in ε and use it together with (2) in (1) to find the following form of the system, which is investigated in this study:

$$\begin{aligned} R &= \exp\{\varepsilon[1 - \exp(-\alpha t)]\} \\ &= 1 + \varepsilon[1 - \exp(-\alpha t)] + 0(\varepsilon^2) \\ &= 1 + \varepsilon - \varepsilon \exp(-\alpha t) + 0(\varepsilon^2) \end{aligned} \quad (4a)$$

Consider equations (3a-e), for equation (3e) we use (3a).

In order to reduce the system of partial differential equations above to a system of ordinary differential equations in dimensionless form, we represent the linear velocity, pressure and concentration as:

$$u(r, t) = u_0(r) + \varepsilon(1 - e^{-\alpha t})u_1(r) + 0(\varepsilon^2) \quad (5a)$$

$$P(r, t) = P_0(r) + \varepsilon(1 - e^{-\alpha t})P_1(r) + 0(\varepsilon^2) \quad (5b)$$

$$C_1(r, t) = C_{10}(r) + \varepsilon(1 - e^{-\alpha t})C_{11}(r) + 0(\varepsilon^2) \quad (5c)$$

$$C_2(r, t) = C_{20}(r) + \varepsilon(1 - e^{-\alpha t})C_{21}(r) + 0(\varepsilon^2) \quad (5d)$$

First, we solve steady state components:

$$\frac{\partial P_0}{\partial r} = u_0, \quad (5e)$$

$$\frac{\partial u_0}{\partial r} = a_1 - a_2 P_0, \quad (5f)$$

$$\frac{u_0 \partial C_{10}}{\partial r} = D_1 \left[\left(\frac{1}{r^2} \right) \left(\frac{\partial}{\partial r} \right) \left(\frac{r^2 \partial C_{10}}{\partial r} \right) \right] - a_3 C_{10} - a_4 C_{20} \quad (5g)$$

$$\frac{u_0 \partial C_{20}}{\partial r} = D \left[\left(\frac{1}{r^2} \right) \left(\frac{\partial}{\partial r} \right) \left(\frac{r^2 \partial C_{20}}{\partial r} \right) \right] - a_5 C_{10} - a_6 C_{20} \quad (5h)$$

$$\frac{\partial P_0}{\partial r} = 0 \text{ at } r = 0 \quad (5i)$$

$$P_0 = P_B, C_{i0} = C_{Bi}, \partial C_{i0} / \partial r = T_i \text{ at } r = 1, (i = 1, 2), \quad (5j)$$

Using (5f)-(5g) and (5j)-(5k), we find the following analytical solutions for the steady state velocity and pressure

$$P_0(r) = (a_1/a_2) + [P_B - (a_1/a_2)] \cos[a_2^{1/2} r] / \cos[a_2^{1/2}], \quad (6a)$$

$$u_0(r) = -(a_2)^{-5} + [P_B - (a_1/a_2)] \sin[(a_2)^{1/2} r] / \cos[(a_2)^{1/2}], \quad (6b)$$

For unsteady components, we have

$$\frac{\partial P_1}{\partial r} = u_1, \quad (6c)$$

$$\frac{\partial u_1}{\partial r} = -a_2 P_1, \quad (6d)$$

$$-\alpha C_{11} + u_0 \frac{\partial C_{11}}{\partial r} + \frac{u_1 \partial C_{10}}{\partial r} \quad (6e)$$

$$= D_1 \left[\left(\frac{1}{r^2} \right) \left(\frac{\partial}{\partial r} \right) \left(\frac{r^2 \partial C_{11}}{\partial r} \right) \right] - a_3 C_{11} - a_4 C_{21}$$

$$-\alpha C_{21} + u_0 \frac{\partial C_{21}}{\partial r} + \frac{u_1 \partial C_{20}}{\partial r} \quad (6f)$$

$$= L_2 \left[\left(\frac{1}{r^2} \right) \left(\frac{\partial}{\partial r} \right) \left(\frac{r^2 \partial C_{21}}{\partial r} \right) \right] - a_5 C_{11} - a_6 C_{21}$$

$$P_1 = -\frac{\partial P_0}{\partial r} \text{ at } r = 1 \quad (6g)$$

$$\frac{\partial P_1}{\partial r} = 0 \text{ at } r = 0 \quad (6h)$$

$$C_{i1} = -\frac{\partial C_{i0}}{\partial r} \text{ at } r = 1, (i = 1, 2), \quad (6i)$$

$$\frac{\partial C_{i1}}{\partial r} = -\frac{\partial^2 C_{i0}}{\partial r^2} \text{ at } r = 1, (i = 1, 2), \quad (6j)$$

From (6a-b), we have

$$\frac{\partial^2 P_1}{\partial r^2} = -a_2 P_1 \quad (7a)$$

$$P_1 = \frac{[P_B - a_1/a_2] \sqrt{a_2} \tan[\sqrt{a_2}]}{\cos(\sqrt{a_2})} \cos(\sqrt{a_2} r)$$

$$u_1 = \frac{-a_2 [P_B - a_1/a_2] \tan[\sqrt{a_2}]}{\cos(\sqrt{a_2})} \sin(\sqrt{a_2} r) \quad (7b)$$

We make the governing system of equations dimensionless using length scale R_0 , time scale R_0^2/ν , where $\nu = \mu/\rho$ is kinematic viscosity and ρ is fluid density, velocity scale ν/R_0 and pressure scale $\nu^2 \rho/k$, so that the dimensional forms of the variables and R are related to their non-dimensional counterpart by

$$\begin{aligned} &(\tilde{r}, \tilde{t}, \tilde{u}, \tilde{P}, \tilde{R}) \\ &= \left[R_0 r, \left(R_0^2 / \nu \right) t, (\nu / R_0) u, (\nu^2 \rho / k) P, R_0 R \right] \end{aligned} \quad (8)$$

$$b_i = a_i R_0^2 / \nu \quad (i = 1, 3, 4, 5, 6),$$

$$b_2 = a_2 \nu R_0^2 / k, P_B = \tilde{P}_B k / (\rho \nu^2) \text{ and } T_i = \tilde{T}_i R_0$$

It should be noted that our non-dimensional procedure makes quantities of interest just dimensionless, so that the results can be applicable to a wide range of cases and biomedical problems in the subject area of this paper. After the variables are non-dimensionalized, we have

$$P_0(r) = (b_1/b_2) + [P_B - (b_1/b_2)] \cos[b_2^{1/2} r] / \cos[b_2^{1/2}], \quad (9a)$$

$$u_0(r) = -(b_2)^{-5} + [P_B - (b_1/b_2)] \sin[b_2^{1/2} r] / \cos[b_2^{1/2}], \quad (9b)$$

$$\frac{\partial P_0}{\partial r} = u_0, \quad (9c)$$

$$\frac{\partial u_0}{\partial r} = b_1 - b_2 P_0, \quad (9d)$$

$$\frac{u_0 \partial C_{10}}{\partial r} = L_1 \left[\left(\frac{1}{r^2} \right) \left(\frac{\partial}{\partial r} \right) \left(r^2 \frac{\partial C_{10}}{\partial r} \right) \right] - b_3 C_{10} - b_4 C_{20} \quad (9e)$$

$$\frac{\partial C_{i1}}{\partial r} = -\frac{\partial^2 C_{i0}}{\partial r^2} \text{ at } r=1, (i=1, 2), \quad (10j)$$

$$\frac{u_0 \partial C_{20}}{\partial r} = L_2 \left[\left(\frac{1}{r^2} \right) \left(\frac{\partial}{\partial r} \right) \left(r^2 \frac{\partial C_{20}}{\partial r} \right) \right] - b_5 C_{10} - b_6 C_{20} \quad (9f)$$

$$\frac{\partial P_0}{\partial r} = 0 \text{ at } r = 0 \quad (9g)$$

$$P_0 = P_B, C_{i0} = C_{Bi}, \partial C_{i0} / \partial r = T_i \text{ at } r=1, (i=1, 2), \quad (9h)$$

$$\frac{\partial^2 P_1}{\partial r^2} = -b_2 P_1 \quad (10a)$$

$$P_1 = \frac{[P_B - b_1/b_2] \sqrt{b_2} \tan[\sqrt{b_2}]}{\cos(\sqrt{b_2})} \cos(\sqrt{b_2} r)$$

$$u_1 = \frac{-b_2 [P_B - b_1/b_2] \tan[\sqrt{b_2}]}{\cos(\sqrt{b_2})} \sin(\sqrt{b_2} r) \quad (10b)$$

$$\frac{\partial P_1}{\partial r} = u_1, \quad (10c)$$

$$\frac{\partial u_1}{\partial r} = -b_2 P_1, \quad (10d)$$

$$-\alpha C_{11} + u_0 \frac{\partial C_{11}}{\partial r} + \frac{u_1 \partial C_{10}}{\partial r} \quad (10e)$$

$$= L_1 \left[\left(\frac{1}{r^2} \right) \left(\frac{\partial}{\partial r} \right) \left(r^2 \frac{\partial C_{11}}{\partial r} \right) \right] - b_3 C_{11} - b_4 C_{21}$$

$$-\alpha C_{21} + u_0 \frac{\partial C_{21}}{\partial r} + \frac{u_1 \partial C_{20}}{\partial r} \quad (10f)$$

$$= L_2 \left[\left(\frac{1}{r^2} \right) \left(\frac{\partial}{\partial r} \right) \left(r^2 \frac{\partial C_{21}}{\partial r} \right) \right] - b_5 C_{11} - b_6 C_{21}$$

$$P_1 = -\frac{\partial P_0}{\partial r} \text{ at } r=1 \quad (10g)$$

$$\frac{\partial P_1}{\partial r} = 0 \text{ at } r = 0 \quad (10h)$$

$$C_{i1} = -\frac{\partial C_{i0}}{\partial r} \text{ at } r=1, (i=1, 2), \quad (10i)$$

We calculated the main quantities, the velocity, pressure and the concentrations of two drugs by using the numerical values for the non-dimensional constant coefficients b_i , ($i=1, \dots, 6$); and, for the non-dimensional parameters, L_i and the boundary values P_B , C_{Bi} and T_i ($i=1, 2$). These numerical values are chosen based on the dimensional values of the corresponding quantities, which are primarily collected from the relevant literature on biomedical applications [10,12,20]. The non-dimensional values of the constant coefficients b_i , ($i=1, \dots, 6$), boundary values are P_B , C_{Bi} and T_i ($i=1, 2$), and the diffusion parameters L_i ($i=1, 2$) are given in Table 1 [19]. For the two anticancer drugs, we choose etanidazole, which is used for radiotherapy, and cisplatin, which is a kind of chemotherapy drug using (10) in (10e-f), we numerically solve these second order differential equations subjected to the boundary conditions given in (10i-j) by an efficient Runge-Kutta fourth order and obtain C_{10} , C_{11} , C_{20} and C_{21} (for completeness we have included Table1 and the definitions for all constants).

Table 1. Non-dimensional values of the quantities that are used in the calculation

Quantities	Tumor values	Normal tissue values	Cavity values
b_1	-4.436064(10 ⁻¹¹)	-5.84496(10 ⁻¹²)	
b_2	8.44(10 ⁻¹¹)	1.08 (10 ⁻¹¹)	
b_3	3.32(10 ⁻⁴)	0.424(10 ⁻⁴)	0.424(10 ⁻⁴)
b_4	0.03324(10 ⁻⁴)	0.00424(10 ⁻⁴)	0.00424(10 ⁻⁴)
b_5	3.32(10 ⁻⁴)	0.424(10 ⁻⁴)	0.424(10 ⁻⁴)
b_6	0.03324(10 ⁻⁴)	0.00424(10 ⁻⁴)	0.00424(10 ⁻⁴)
C_{B1}	0.1(10 ⁻³)	0.1(10 ⁻³)	0.1(10 ⁻³)
C_{B2}	0.1(10 ⁻³)	0.1(10 ⁻³)	0.1(10 ⁻³)
L_1	1.4175(10 ⁻⁵)	0.525(10 ⁻⁶)	0.3003(10 ⁻⁵)
L_2	1.4175(10 ⁻⁸)	0.525(10 ⁻⁸)	0.3003(10 ⁻⁸)
P_B	1.84(10 ⁻³)	1.84(10 ⁻³)	1.84(10 ⁻³)
T_1	0.1(10 ⁻²)	0.1(10 ⁻²)	0.1(10 ⁻²)
T_2	0.1(10 ⁻²)	0.1(10 ⁻²)	0.1(10 ⁻²)

3. Results and Discussions

3.1. Pressure

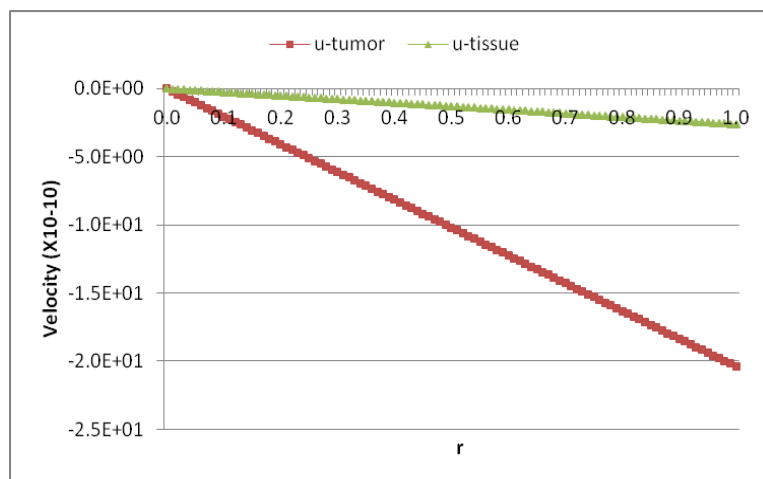


Figure 1. interstitial pressure versus radial variable for tumor and normal tissue

The non-dimensional interstitial pressure is calculated in terms of trigonometric function. Figure 1 presents pressure versus the radial variable for both tumor and normal tissue using equations (5c, 9a and 10a, $\alpha = 1$ and $t = 1$). It can be seen from this figure that the value of the pressure in the tumor is higher than in the tissue, and, also, the pressure decreases as the radius increases; meaning that maximum pressure is found at the center of tumor core ($r = 0$). The radial rate of change of pressure in the tumor is much higher than the corresponding one in the tissue. Our results for both interstitial pressure and velocity agree qualitatively with the available experimental results [5,21,23,24].

3.2. Radial Velocity

The non-dimensional radial velocity is calculated in terms of trigonometric function. Figure 2 presents interstitial radial velocity of the flow versus the radial variable for both tumor and normal tissue using equations (5b, 9b, and 10b $\alpha = 1$ and $t = 1$). Radial velocity is negative because flow enters into the tumor or tissue from the boundary surface. The velocity profile appears to be linear in the sphere for r ($0 < r < 1$), and its magnitude for the tumor is higher than the tissue. It is also seen that $|u| \rightarrow 0$ as $r \rightarrow 0$, which is reasonable since the high interstitial pressure at the center put the motion into rest there. It should be noted that, even though the shape of the velocity is linear, the linearity of the velocity profile is due to the relatively very small values of the velocity that appear to be linear over the short radial distance from 1 to 0.

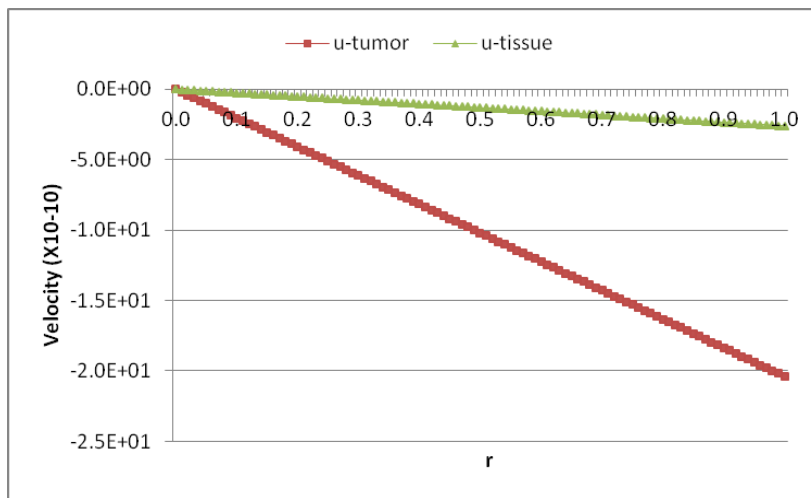


Figure 2. Radial Velocity versus radial variable for tumor and normal tissue

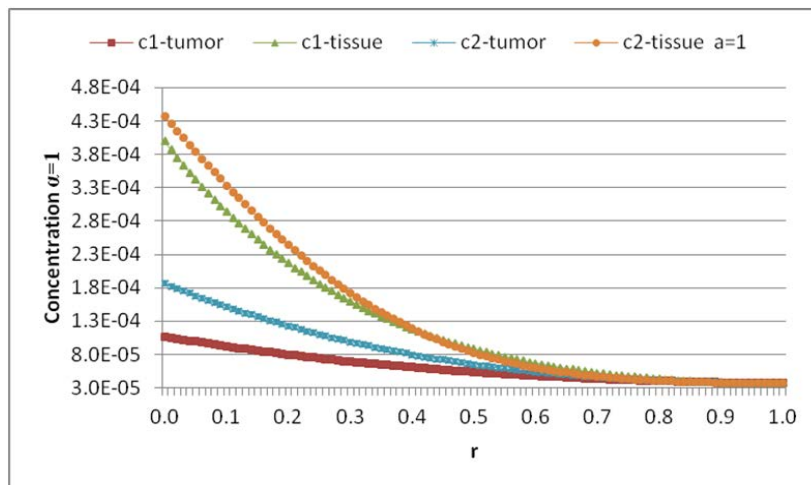


Figure 3. Etanidazole (C1) and Cisplatin (C2) concentration versus radial variable in the absence of the other drugs when $\alpha = 1$, time $t = 1$

3.3. Concentration without Interaction between Two Drugs

First, we only considered the presence of one anti cancer drug, i.e., in the absence of any drug interactions. Results are presented in Figures-3-7. Figure 3 and Figure 4 present concentrations of etanidazole (C_1) and cisplatin (C_2) versus the radial variable for the cases of tumor and normal tissue for $\alpha = 1$ and $\alpha = 3$ at time $t = 1$ using

equations (5d, 5e, 9e, 9f, 10e, 10f). We can see from these figures that the concentrations of both drugs increased when the radius decreased and reached a maximum at $r = 0$. The value of concentration in the tumor is less than in the tissue. The radial rate of change of the concentration is highest in the tissue and is lowest in the tumor. For a given value of the radius, the value of the concentration for cisplatin (C_2) is found to be higher than that for the etanidazole (C_1). This is due to the smaller value of the diffusion parameter L_2 as compared to the value of the diffusion parameter L_1 [25]. The results for the radial

variations of the concentrations indicate that the concentrations close to $r = 1$ have smaller radial rates of increase when compared to their rate of increase near the center. We observe that, as the growth rate of the tumor increases (as the value of α increases from 1 to 3), the magnitude of the concentration decreases, although the

shape of the concentration profile remains the same. Thus drug delivery in a tumor is inversely proportional to the growth rate, which is reasonable. We also calculated the drug concentration for different initial loading and found that the values of the concentration increased with increased loading.

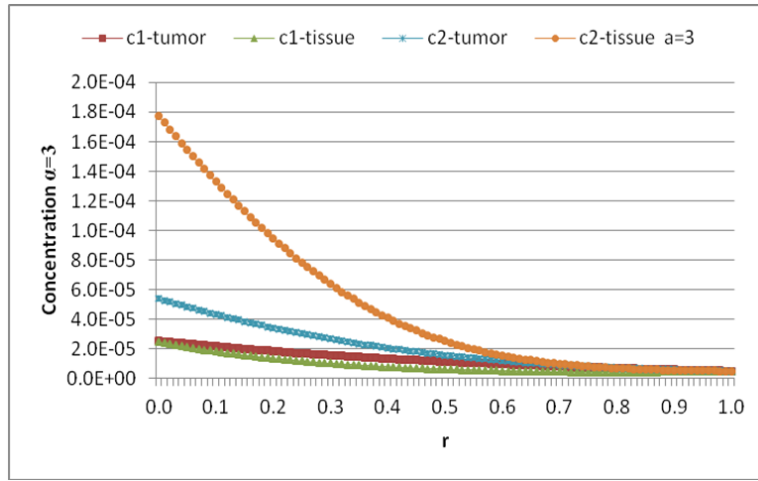


Figure 4. Etanidazole (C1) and Cisplatin (C2) concentration versus radial variable in the absence of the other drugs when $\alpha = 3$, time $t = 1$

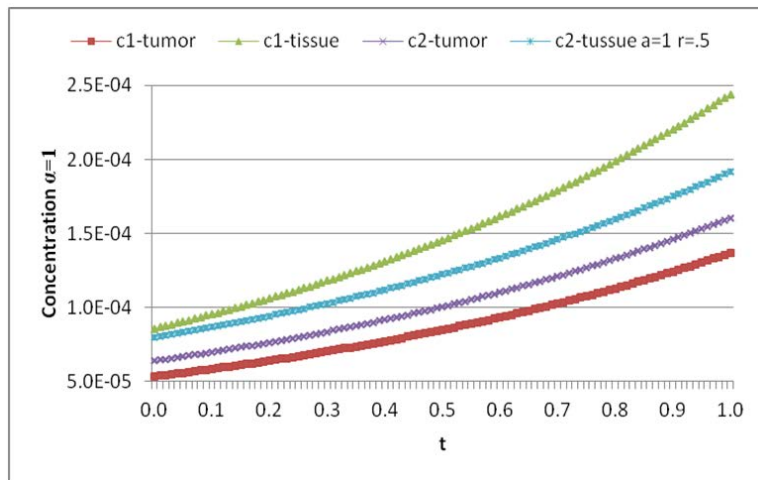


Figure 5. Etanidazole (C1) and Cisplatin (C2) concentration versus time in the absence of the other drugs when $\alpha = 1$ and $r = 0.25$

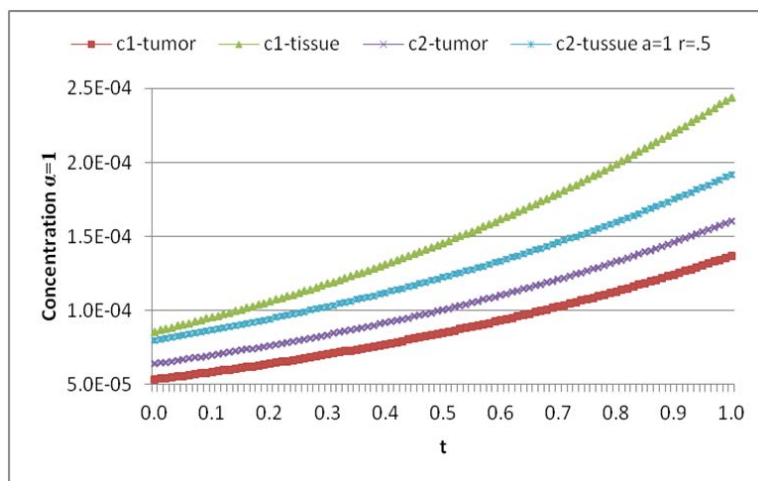


Figure 6. Etanidazole (C1) and Cisplatin (C2) concentration versus time in the absence of the other drugs when $\alpha = 1$ and $r = 0.5$

Figure 5, Figure 6, Figure 7 show the concentrations of C_1 (etanidazole) and C_2 (cisplatin) versus the time variable for the cases of tumor and normal tissue at

different locations $r = .25$, $r = .5$ and $r = .75$ for different values $\alpha = 1$ and 3 (for brevity only $\alpha = 1$ is presented). The shape of all of the curves is similar, that is, they start

form the axis with the minimum and increase as the time increases and attaining the maximum at $t = 1$. It should be noted that, due to the periodicity of the flow, all the results presented for the quantities versus t repeat as a new cycle in time begins. The rate of change of the concentration is highest in the tissue and is lowest in the tumor. The variations of the concentrations indicate that the concentrations close to $t = 1$ have a higher rate of increase when compared to the rate of increase at the beginning. At the beginning ($t = 0$), the concentrations are very small

and increased slowly over time. As a result, it is not unexpected that the anti cancer drugs take a long time to penetrate the tumor. It is observed that the magnitudes of concentrations higher at $r = 0.25$ than those at $r = 0.5$ and $r = 0.75$, and the magnitudes of the concentrations higher at $r = 0.5$ than at $r = 0.75$. The maximum concentration occurs near the center of the tumor. This indicates that the maximum concentration is at the core region and rises as a function of time.

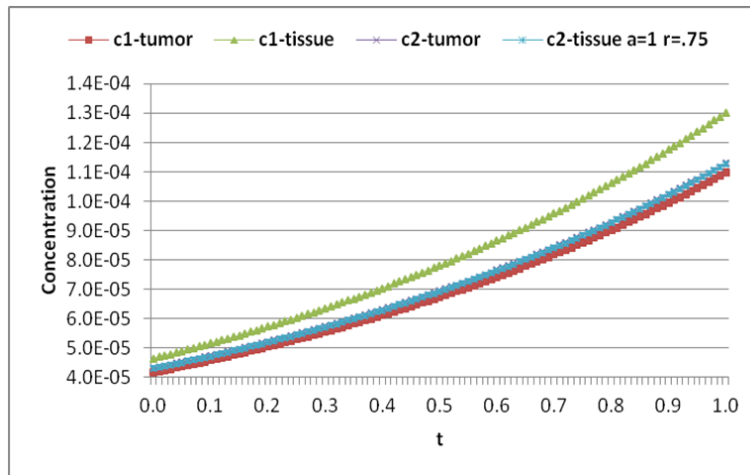


Figure 7. Etanidazole (C1) and Cisplatin (C2) concentration versus time in the absence of the other drugs when $\alpha = 1$ and $r = 0.75$

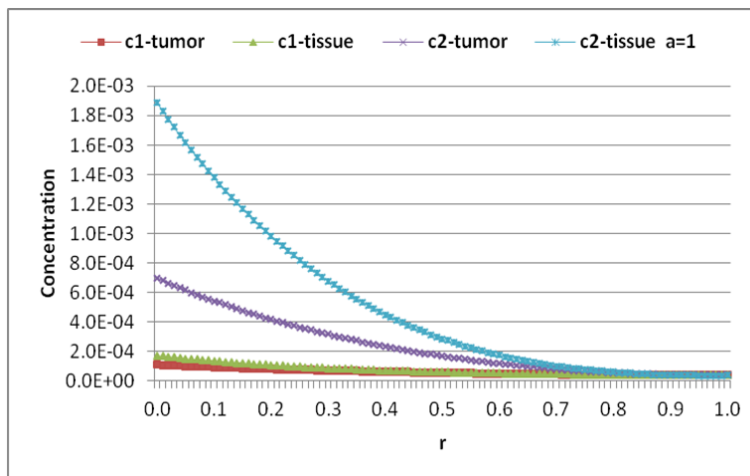


Figure 8. Etanidazole (C1) and Cisplatin (C2) concentration versus radial variable in the presence of the other drugs when $\alpha = 1$, time $t = 1$

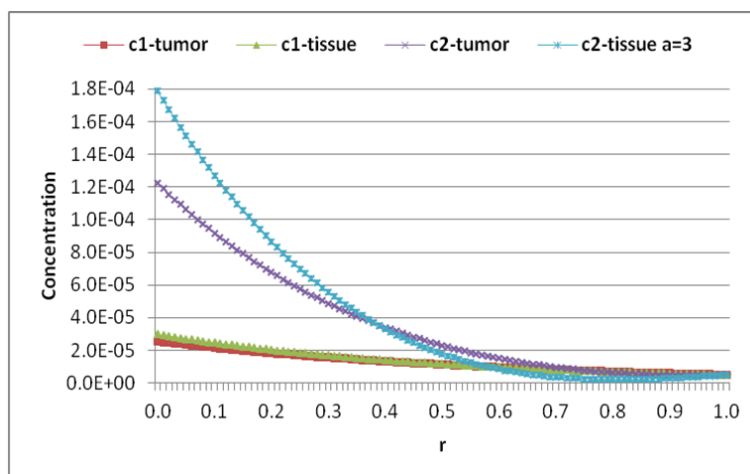


Figure 9. Etanidazole (C1) and Cisplatin (C2) concentration versus radial variable in the presence of the other drugs when $\alpha = 3$ time $t = 1$

3.4. Concentration with Interaction between Two Drugs

We calculate the concentrations of drugs when both drugs are present and some of our results for such cases are shown in Figure 8 and Figure 12. Figure 8 and Figure 9 present concentrations of etanidazole (C_1) and cisplatin (C_2) versus the radial variable for the cases of tumor and normal tissue for $\alpha = 1$ and 3 at time $t = 0$ using equation (5d, 5e, 9e, 9f, 10e, 10f). These figures implied that both concentrations increase as the radius decreases. The radial rate of change of concentration is highest in the normal tissue and lowest in the tumor, and the value of concentration in the normal tissue is higher than in the tumor. The value of the concentration of cisplatin is higher than that of etanidazole at a given radius. As before, we observe that, as the growth rate of the tumor increase (as the value of α increased from 1 to 3), the magnitude of the

concentration decreases; although the shape of the concentration profile remains the same. Similar to the case in the absence of drug interaction presented in Figure 3, and Figure 4, we can see from Figure 8, and Figure 9 that the radial rate of change of each of these concentrations is higher close to the center. Comparing the results in Figure 8, and Figure 9 to those in Figure 3, and Figure 4, we found that the values of the concentrations increase as a result of the presence of both the concentrations in the tumor and in the tissue.

Figure 10, Figure 11 and Figure 12 represent the concentrations of C_1 (etanidazole) and C_2 (cisplatin) versus the time variable at different locations $r = .25$, $r = .5$ and $r = .75$ for different values $\alpha = 1$ and 3 (for brevity only $\alpha = 1$ is presented). The shape of all the curves is similar, that is, they start from the axis ($t = 0$) with a minimum and increases as the time increases and attaining a maximum at $t = 1$.

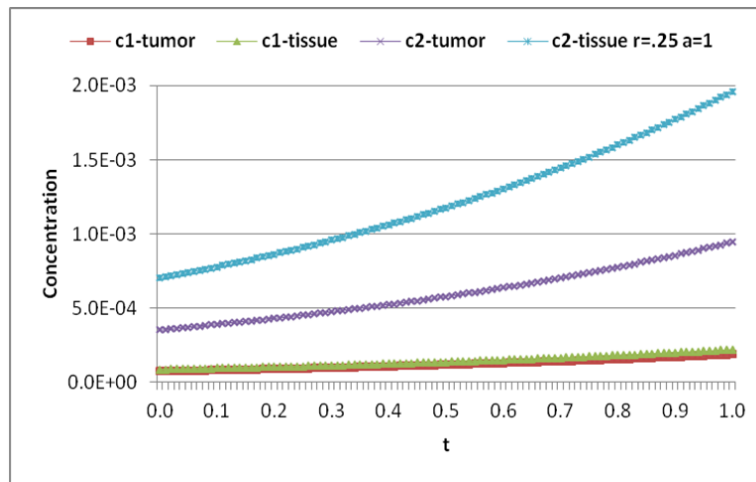


Figure 10. Etanidazole (C_1) and Cisplatin (C_2) concentration versus time in the presence of the other drugs when $\alpha = 1$ and $r = 0.25$

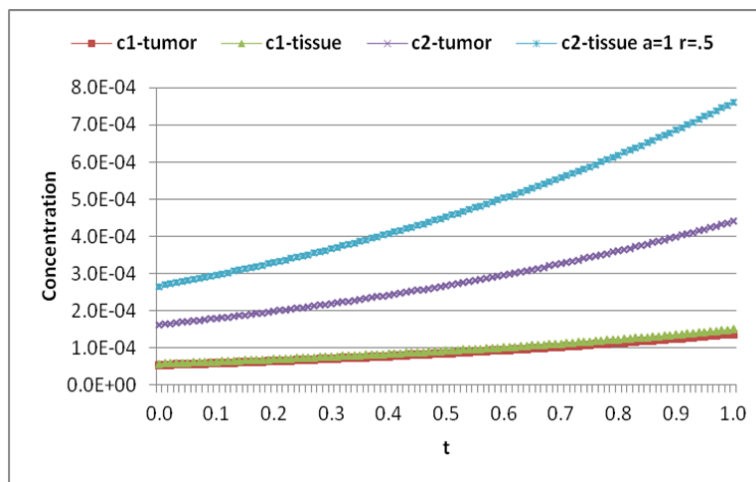


Figure 11. Etanidazole (C_1) and Cisplatin (C_2) concentration versus time in the presence of the other drugs when $\alpha = 1$ and $r = 0.5$

Similar to the case in the absence of drug interaction presented in Figure 5, Figure 6 and Figure 7, the rate of change of the concentration is the highest in the tissue and is the lowest in the tumor. The variations of the concentrations indicate that the concentrations close to $t = 1$ has higher rates of increase when compared to their rate of increase at the beginning ($t = 0$). As before, at the beginning ($t = 0$), the concentrations are very small and

increase slowly with time. It shows that the anticancer drugs take a long time to penetrate into a tumor. It is observed that the magnitudes of concentrations are higher at $r = 0.25$ than those at $r = 0.5$ and $r = 0.75$ and also that the magnitude of concentrations are higher at $r = 0.5$ than those at $r = 0.75$. The maximum concentration occurs near the center of the tumor. Comparing the values of the concentrations of two anti cancer drugs with interaction

(Figures 8-12) and without interaction (Figures 3-7), we observe that the values of the concentrations increase with interaction both in the tumor and in the normal tissue. This result reveals that, in a real drug delivery system to

patients, giving a secondary drug to the patients could slightly help to increase the amount of the primary and secondary drugs deliver to a patient's tumor, thereby improving the patient's health conditions.

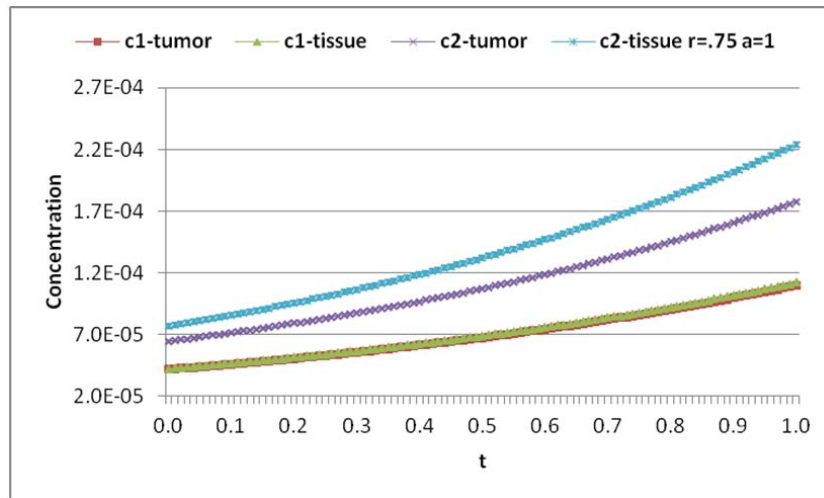


Figure 12. Etanidazole (C1) and Cisplatin (C2) concentration versus time in the presence of the other drugs when $\alpha = 1$ and $r = 0.75$

The efficacy of a drug delivery system defined by Tan *et al.* [12] is that, for a given radius, it can depend on the ratio between values of the concentration in the tumor to those in normal tissue. This ratio is referred to as the Therapeutic Index (TI) in relevant biomedical literature. Thus TI is a measure of the efficiency of the drug delivery, so that a higher value of TI indicates that a higher amount of drug is delivered to the tumor than to the normal tissue. In our results for the concentrations of etanidazole and cisplatin presented in Figures 3-12, we concluded that, for either etanidazole or cisplatin, TI is greater in the presence of one drug in the system.

The following observations are made:

- (i) The pressure is highest at the center of the tumor and decreases towards the border of the tumor;
- (ii) The magnitude of the radial fluid velocity predicted by the model is lowest at the center of the tumor and increases towards the periphery;
- (iii) The concentration of the two anticancer drugs is higher at the center of the tumor than the periphery;
- (iv) The concentration of both etanidazole and cisplatin is lower in the tumor region than in the normal tissue;
- (v) The concentration near the center of the core region increases faster than near the border region over time;
- (vi) The concentration is higher in the tumor when there is an interaction between the two drugs than when there is no interaction; and,
- (vii) As the growth rate of the tumor increases (as the value of α increases from 1 to 3) the magnitude of the concentration decreases even though the shape of the concentration profile remains the same.

4. Conclusions

Blood flow in a brain tumor is investigated by developing convective-diffusion models for a spherical tumor under the assumption that the growth rate of the tumor is sufficiently small compared to the time scale for the differential equation. We presented the results for unsteady blood flow with unsteady tumor for the main

quantities such as interstitial pressure, unidirectional interstitial velocity and concentrations of two anticancer drugs (etanidazole and cisplatin). We found that the interstitial pressure decreases as the radius increases and maximum pressure is at the center of tumor core; while the magnitude of the interstitial velocity increases when the radial distance increases. The results show that the rate of change of the concentration is highest in the tissue and lowest in the tumor. The variations of the concentrations indicate that the rate of concentration increases as the time increases, i.e., at the beginning ($t = 0$) the concentrations are very small and increase slowly with time. This shows that anti center drugs take a long time to penetrate into a tumor. These results appear to agree qualitatively with the available experimental results. We also calculated the values of concentrations of two drugs in the presence or absence of a second drug and observed that presence of both drugs can improve the amount of the drug in the flow system. This result also indicates that non-trivial cases can be investigated theoretically to discover ways that can improve drug delivery to the patient.

In this study, we carried out investigations and calculations for cases with unsteady blood flow and an unsteady homogeneous tumor. We presented results for the unsteady cases including, specifically, those affected by the growth rate of the tumor and how much growth rate can be controlled by drug delivery mechanisms. In the future, the theoretical model developed in this paper will be extended further to apply to non-unidirectional tumors and tissues in terms of properties and geometrical configurations. In addition, we will broaden our model to predict the effect on the tumor growth due to the rate of drug delivery to the tumor for the actual operating and drug conditions in medical cases for a brain tumor.

Acknowledgements

This research has been supported by a "Faculty Research Council" (FRC-UTPA) grant during the academic year 2011-2012.

References

- [1] G. Powathi, M. Kohandel, S. Sivaloganathan, A. Oza and M. Milosevic, Mathematical modeling of brain tumors: effects of radiotherapy and chemotherapy, *Phys. Med. Biol.* 52 3291-3306 (2007).
- [2] L. Barazzuol, NG. Burnet, R Jena, B. Jones, SJ. Jefferies, NF. Kirkby, A mathematical model of brain tumor response to radiotherapy and chemotherapy considering radiobiological aspects, *Journal of Theoretical Biology*, 262, 553-565, (2010).
- [3] R. K. Jain, Barriers to drug delivery in solid tumors, *Sci Am* 271, 58-65, (1994).
- [4] R. K. Jain, Normalization of tumor vasculature: An emerging concept in antiangiogenic therapy. *Science* 307, 58-62, (2005).
- [5] L. T. Baxter, R. K. Jain, Transport of fluid and macromolecules in tumors. (I) role of interstitial pressure and convection. *Microvasc. Res.* 37, 77-104, (1989).
- [6] L. T. Baxter, T., R. K. Jain, Transport of fluid and macromolecules in tumors. (II) role of heterogeneous perfusion and lymphatics. *Microvasc. Res.* 40, 246-263, (1990).
- [7] L. T. Baxter, R. K. Jain, Transport of fluid and macromolecules in tumors. (III) role of binding and metabolism. *Microvasc. Res.* 41, 5-23, (1991).
- [8] C. H. Wang, J. Li, Three dimensional iggs delivery to tumors. *Chemical Eng. Science* 53, 3579-3600, (1998).
- [9] J. Zhao, H. Salmon, M. Sarntinoranont, Effect of heterogeneous vasculature on interstitial transport within a solid tumor. *Microvasc. Res.* 73, 224-236, (2007).
- [10] M. Soltani, P. Chen, Numerical modeling of fluid flow in solid tumors. *Plos One* 6, issue 6, e20344, (2011).
- [11] W. M. Saltzman, M. L. Radomsky, Drugs released from polymers: diffusion and elimination in brain tissue. *Chemical Eng. Science* 46, 2429-2444, (1991).
- [12] W. H. K. Tan, F. J. Wang, T. Lee, C. H. Wang, Computer simulation of the delivery of etanidazole to brain tumor from PLGA wafers: Comparison between linear and double burst release systems. *Biotechnology and Bioengineering* 82, 278-288, (2003).
- [13] C. S. Teo, W. Tan, H. K., Lee, T., Wang, C. H, Transient interstitial fluid flow in brain tumors: Effects on drug delivery. *Chemical Eng. Science* 60, 4803-4821, (2005).
- [14] D. Y. Arifin, K. Y. Lee, C. H. Wang, Chemotherapeutic drug transport to brain tumor. *J. Control Release*, 137, 203-210, (2009).
- [15] J. Sinek, H. Frieboes, X. Zheng, V. Cristini, Two-dimensional chemotherapy simulations demonstrates fundamental transport and tumor response limitations involving nanoparticles. *Biomed. Microdevices.* 6(4), 297-309 (2004).
- [16] X. Zheng, SM, Wise, V. Cristini, Nonlinear simulation of tumor necrosis, neo-vascularization and tissue invasion via an adaptive finite-element/level-set method. *Bull. Math. Biol.* 67, 211-259, (2005).
- [17] K. R. Swanson, , E. C. Alvord, J. D. Murray, Virtual brain tumors (gliomas) enhance the reality of medical imaging and highlight inadequacies of current therapy, *British J. Cancer* 86, 14-18, (2002).
- [18] S. E. Eikenberry, T. Sankar, MC. Preul; EJ; Kostelich, CJ Thalhauser, Y. Kuang,, Virtual glioblastoma: growth, migration and treatment in a three-dimensional mathematical model, *Cell Proliferation*, 42, 511-528, (2009).
- [19] D. N Riahi and R. Roy, Mathematical modeling of fluid flow in brain tumor, under review, (2012).
- [20] R. K. Jain, L. T. Baxter, Mechanisms of heterogeneous of monoclonal anti-bodies and other macromolecules in tumors: significance of elevated interstitial pressure. *Cancer Res.* 48, 7022-7032, (1988).
- [21] R. K. Jain, Transport of molecules in the tumor interstitium: A review. *Cancer Res.* 47, 3039-3051, (1987).
- [22] J. W. Baish, P. A. Netti, R. K. Jain, Transmural coupling of fluid flow in microcirculatory network and interstitium in tumors , *Microvascular Research*, 53, 128-141, (1997).
- [23] Y. Boucher, Baxter, L. T, Interstitial pressure gradients in tissue-isolated and subcutaneous tumors: Implication for therapy. *Cancer Res.* 50, 4478-4484, (1990).
- [24] R. K. Jain, R. T. Tong, L. L. Munn, Effect of vascular normalization by antiangiogenic therapy on interstitial hypertension, peritumor edema, and lymphatic metastasis. *Cancer Res.* 67, 2729-2735, (2007).
- [25] L. D. Landau, E. M, Lifshitz, Fluid Mechanics, 2nd edition. (1987), Pergamon Press, Oxford.